ACS OMEGA

Article

Cite This: ACS Omega 2018, 3, 1137−1146

Ultrafast Self-Healable Interfaces in Polyurethane Nanocomposites Designed Using Diels−Alder "Click" as an Efficient Microwave Absorber

Aishwarya V. Menon,[†] Giridhar Madras,[‡] and Suryasarathi Bose*[,§]

[†]Center for Nano Science and Engineering, [‡]Department of Chemical Engineering, and [§]Department of Materials Engineering, Indian Institute of Science, Bangalore 560012, India

Supporting Information

ABSTRACT: In the recent times, multifunctional materials have attracted immense interest. Self-healing polymers are in great demand in almost every coating application. With an increase in electromagnetic (EM) pollution, curbing the same has become an urgent necessity. Lightweight coatings and conducting polymeric materials are being highly researched upon in this regard, and combining these properties with self-healing systems would open new avenues in EM interference (EMI) shielding (specifically in the microwave frequency domain) applications. In the current study, a novel approach toward the development of microwave shielding materials capable of self-healing through microwave heating has been attempted. A covalently cross-linked material was developed using Diels−Alder (DA) chemistry, which shows self-healing properties when stimulated by heating. Herein, reduced graphene oxide grafted with magnetite nanoparticles (rGO/Fe_3O_4) was covalently cross-linked to thermoplastic polyurethane using DA chemistry. The addition of multiwalled carbon nanotubes into these nanocomposites led to exceptional EM wave shielding and self-healing properties through a synergistic effect. The synergism led to exceptional EMI shielding of −36 dB, primarily through absorption in the microwave region of the EM spectrum. When used in the form of thin coatings of about 1 mm in thickness, the shielding value reached −28 dB, manifesting in more than 99% attenuation of EM waves through absorption. The material was also found to be capable of healing scratches or cuts through microwave irradiation.

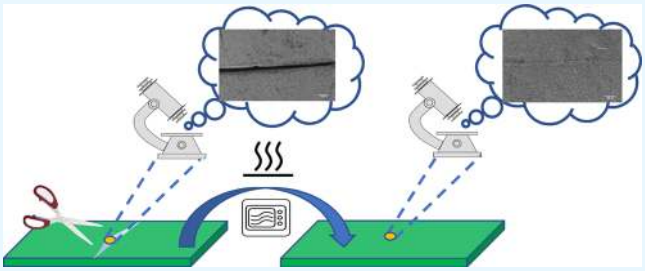

INTRODUCTION

The recent advancements in science and technology have led to pervasive use of electronic devices which emit electromagnetic (EM) radiations as their byproduct. The miniaturization of devices has led to various electric circuitries in a particular device to be placed in close proximity to each other. This invites its own repercussions, leading to interference among these devices causing device malfunctioning. This not only compromises the proper functioning of the devices but also has an adverse effect on human health.[1−3] Therefore, extensive research is being carried out to curb this menace of EM interference (EMI).

EMI can be prevented either by reducing the emission at the source or by immunizing the victim device. The immunization of the victim device is generally achieved by using EMI filters that are local devices used to protect limited number of sensitive elements. Filters pose certain disadvantages, one of which is that they only screen out conducted emissions having characteristics different from that of the device being protected. Therefore, to protect a device from interferences from a broad spectrum of EM waves, there is a pressing need to develop EMI shields. The basic requirements for a shield are good electrical conductivity to reflect EM waves, good magnetic permeability, and the presence of electric and magnetic dipoles to interact with the incoming EM waves and absorb them.

Metals, despite being the most prominent choice as shields, pose several drawbacks such as high density, cumbersome process ability, and poor corrosion resistance. Moreover, there is a demand for flexible and easily moldable materials, which has led to polymer nanocomposites becoming as emerging choices for shielding materials. Polymers are exceptional in the sense that they can be easily customized as per the requirement by adding certain fillers which impart EM shielding properties. Carbonaceous fillers such as carbon black, graphite, graphene, multiwalled carbon nanotubes (MWNTs), carbon fibers, and so forth are highly conducting in nature and can be dispersed in polymer matrices with the ease to develop an EMI shield. Carbonaceous fillers, being electrically conducting in nature, predominantly screen EM waves by reflection, which is not desirable. However, these fillers when used in conjugation with magnetic nanoparticles help in multiple scattering and absorption of EM waves. MWNTs and graphene derivatives

Received: November 23, 2017
Accepted: January 17, 2018
Published: January 26, 2018

DOI: 10.1021/acsomega.7b01845
ACS Omega 2018, 3, 1137−1146

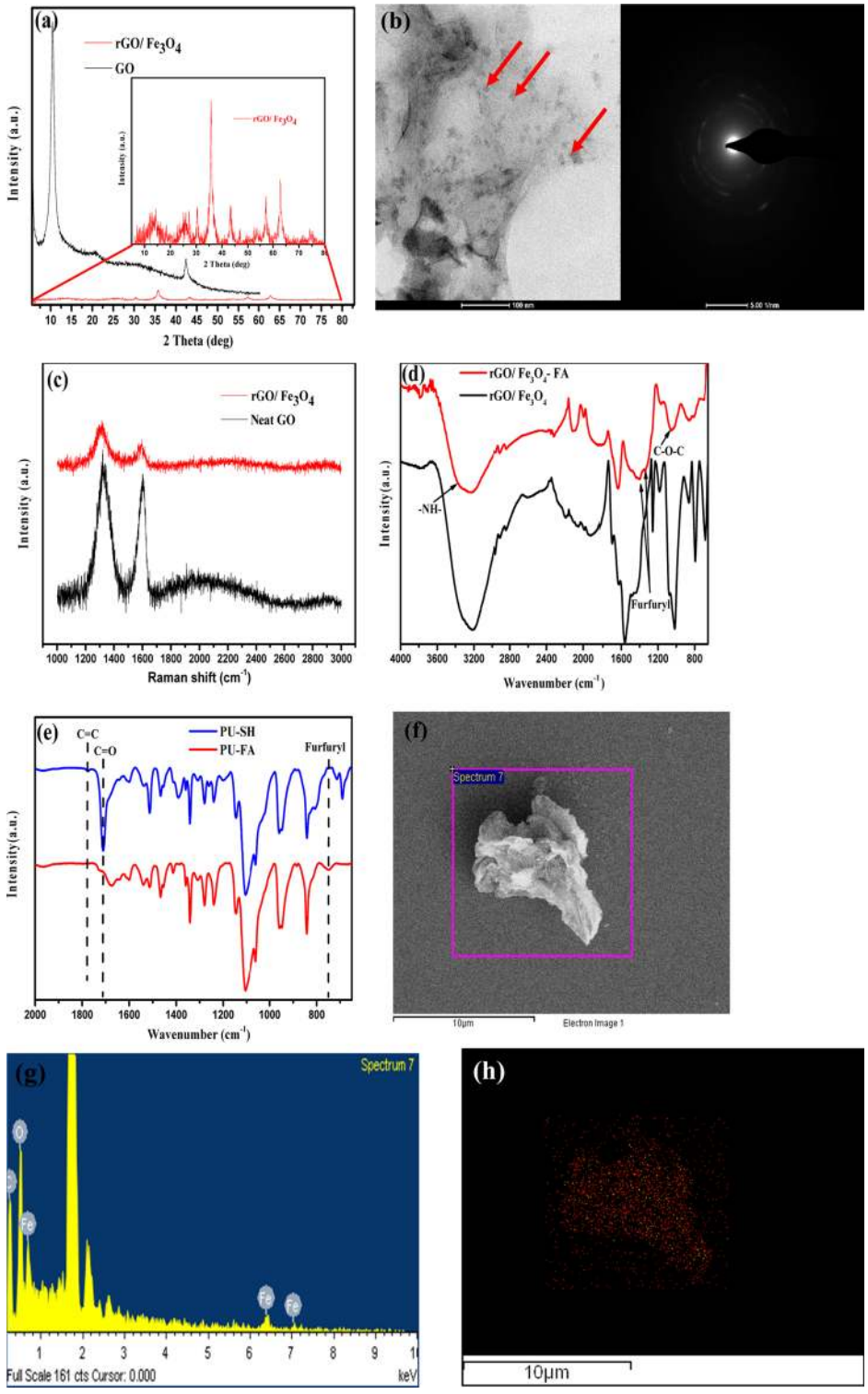

Figure 1. continued

DOI: 10.1021/acsomega.7b01845
ACS Omega 2018, 3, 1137−1146

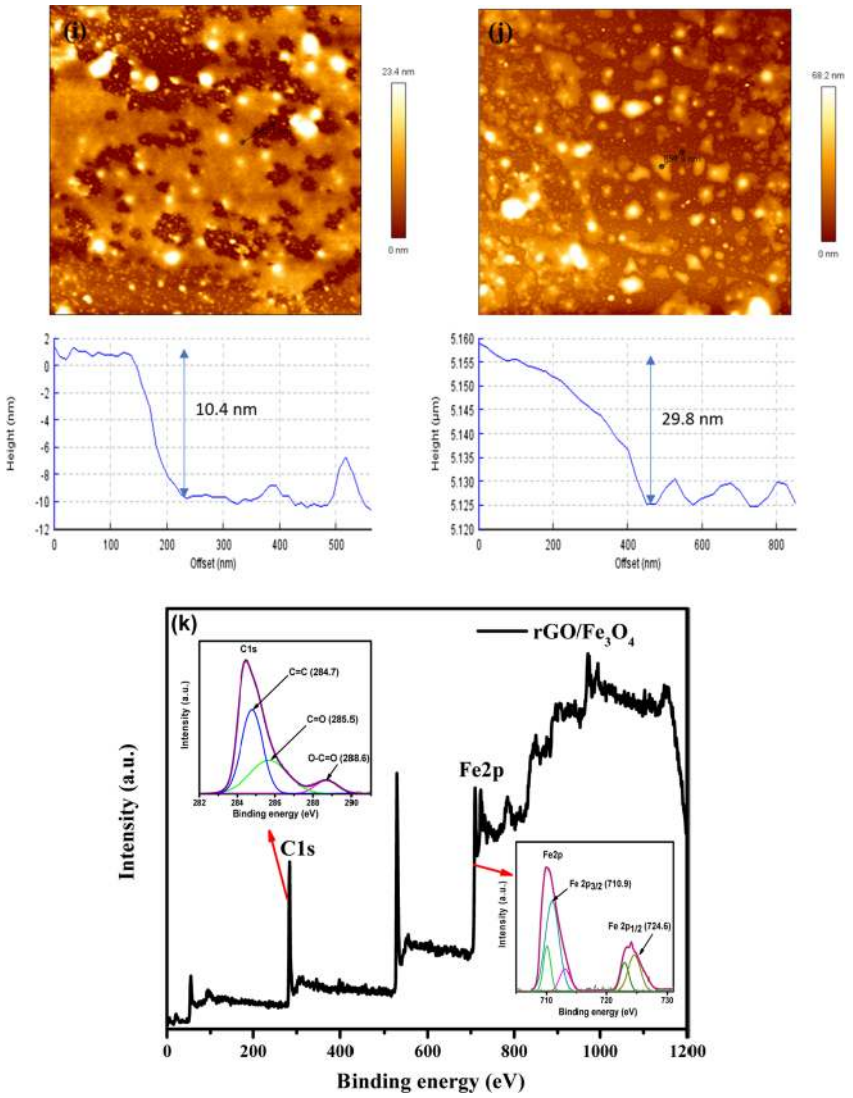

Figure 1. (a) XRD pattern for neat GO and rGO/Fe_3O_4. (b) TEM image and the corresponding SAED pattern of rGO/Fe_3O_4. (c) Raman spectra of neat GO and rGO/Fe_3O_4. (d) FTIR spectrum of rGO/Fe_3O_4 and rGO/Fe_3O_4–FA. (e) FTIR spectrum of PU-FA and PU-SH. (f,g) SEM image and corresponding EDAX spectra of the rGO/Fe_3O_4 sheets. (h) Corresponding EDAX mapping of iron on the rGO sheets. (i) AFM topographic image of neat GO sheets. (j) AFM image of rGO/Fe_3O_4. (k) XPS survey spectra of rGO/Fe_3O_4 along with C 1s and Fe 2p spectra in the inset.

are emerging choices because of their high aspect ratios and skin effect which leads to a high-frequency bandwidth.[4−9]

Graphene oxide (GO) is a versatile material that hosts a large number of functional groups which can be used to graft magnetic particles so that multifunctional materials can be developed for EMI shielding applications. GO is nonconducting in nature, but it can be made conducting by reducing it, forming reduced GO (rGO) which is partially conducting. The planar structure of graphene sheets makes them the ideal choices to graft nanoparticles, thus reducing the percolation concentration of nanoparticles. Grafting of magnetic nanoparticles such as Co, Fe_3O_4, and Ni or dielectric nanoparticles such as $BaTiO_3$ and MnO_2 on rGO sheets helps to improve microwave absorption due to enhanced charge transport and enhanced polarization losses.[10−12] In the light of the above-mentioned facts, we have attempted to conjugate rGO with magnetite nanoparticles using a facile, one-pot approach, solvothermal route. The magnetic nature of these heterostructures when combined with the high conductivity and aspect ratio of MWNTs and dispersed in a polymer matrix helps to develop an excellent EMI shielding material.[13−21]

In an attempt to develop multifunctional materials with more than just one application, we have developed a self-healable EMI shield.[22−32] Self-healable materials are of great interest in this context because the EMI shields may be in the form of coatings which on being scratched can again recover through heating, without losing its shielding properties. These multifunctional materials were developed by cross-linking nanoparticles with the polymer matrix using Diels–Alder (DA) chemistry.[33−37] The nanocomposites developed in this study can be used in the form of thin self-healable coatings for EMI shielding applications. The proposed work represents a novel approach because there is no literature available on EMI shielding materials that are self-healable.

CHARACTERIZATIONS

To characterize the nanoparticles, transmission electron microscopy (TEM) images were acquired using TEM-Titan Themis at 300 kV. The structural properties of the nano-

DOI: 10.1021/acsomega.7b01845
ACS Omega 2018, 3, 1137−1146

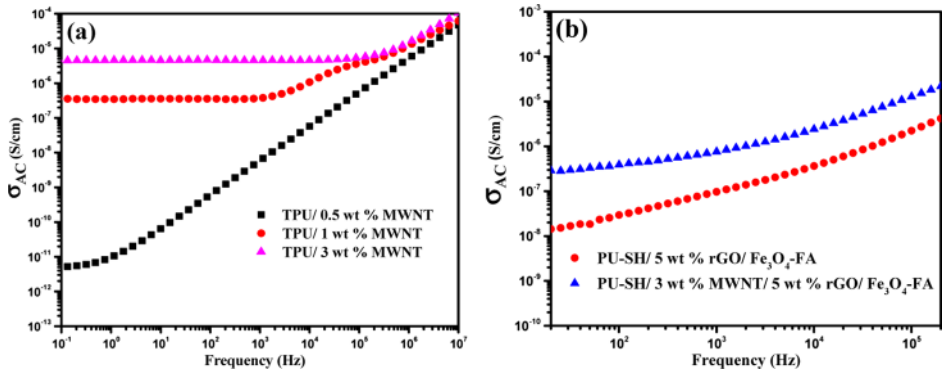

Figure 2. AC electrical conductivity for nanocomposites.

particles were analyzed using an X'pert Pro X-ray diffractometer using a Cu Kα source. The Fourier transform infrared (FTIR) spectra of the samples were recorded using PerkinElmer GX in the range of 4000−650 cm^{-1}, in the ATR mode. The defect characterization of nanoparticles was carried out using a HORIBA LabRAM HR Raman spectrometer. The elemental state of nanoparticles was characterized by an X-ray photoelectron spectrometer (AXIS Ultra) using an Al monochromatic source (1.486 keV). The room-temperature electrical conductivity of the samples was measured on 10 mm compression molded discs using a TA Discovery HR-3 rheometer using a dielectric setup connected to an LCR meter in the frequency range of 20 Hz to 2 MHz. The EMI shielding properties of the as-prepared samples were studied in the X- and Ku-band frequency range using an Anritsu MS4642A vector network analyzer (VNA) using a coax (Damaskos M07T) setup on 5.8 mm thick toroidal specimens, obtained by compression molding. The samples had an outer diameter of 7 mm and inner diameter of 3 mm. The shielding effectiveness (SE) for thin films was measured on a 1 mm thin film using a Keykom waveguide. The healing ability of the nanocomposites was imaged using a ZEISS ULTRA 55 field emission scanning electron microscope with an accelerating voltage of 5 kV.

RESULTS AND DISCUSSION

Characterization of rGO/Fe_3O_4, Furfuryl-Modified rGO/Fe_3O_4, and Furfuryl-Functionalized Polyurethane. Figure 1a represents the X-ray diffraction (XRD) pattern for neat GO and as-synthesised rGO/Fe_3O_4 nanoparticles. Neat GO shows its characteristic peak at 2θ = 10.5°, corresponding to its (001) reflection. After solvothermal functionalization of GO sheets with Fe_3O_4 nanoparticles, six new peaks at 30.4°, 35.7°, 43.4°, 53.7°, 57.4°, and 62.8° can be observed, which corresponds to the (200), (311), (400), (422), (511), and (440) reflections of a cubic spinel structure of pure Fe_3O_4, respectively (JCPDS no. 19-0629).[38] Apart from the characteristic reflections of Fe_3O_4, two broad peaks at 14.3° and 25.4° can be seen, which corresponds to that of the partially reduced GO.[39] Therefore, it can be said that the complete reduction of GO was prevented so that some functional groups can be made available for the functionalization of furfuryl amine (FA) onto GO.

The morphology of rGO/Fe_3O_4 nanoparticles was studied using TEM, as shown in Figure 1b. From the image, it can be seen that small Fe_3O_4 nanoparticles of about 5−10 nm size are dispersed uniformly over the GO sheet. The corresponding selected area electron diffraction (SAED) pattern clearly indicates the polycrystalline nature of these nanoparticles.[40]

The structural changes in the graphitic structure of GO before and after functionalization with Fe_3O_4 nanoparticles were studied using Raman spectroscopy. The I_D/I_G ratio of neat GO and rGO/Fe_3O_4 was found to be 1.07 and 1.70, respectively, as shown in Figure 1c. This shows that the defect concentration increased after solvothermal functionalization because of unpaired defects arising out of the removal of oxygen functional groups.

To determine the successful functionalization of rGO/Fe_3O_4 with FA, FTIR spectra were analyzed, as shown in Figure 1d. In the spectrum of rGO/Fe_3O_4, it can be seen that GO was not completely reduced by the solvothermal process. There are still some functional groups left, such as the peaks at 3220 and 1024 cm^{-1}, corresponding to −OH− and −C−O− stretching vibrations of GO. In the spectrum of rGO/Fe_3O_4−FA, the peak at 3378 cm^{-1} and also the increase in peak broadness due to overlap of −NH− and −OH− stretching vibrations as compared to the spectrum of rGO/Fe_3O_4 shows the presence of the −NH− group from FA. The peaks at 1404 and 1336 cm^{-1} can be assigned to furfuryl, and the peak at 1050 cm^{-1} can be assigned to −C−O−C− of the furfuryl moiety of FA.[41]

The successful completion of the DA reaction and formation of self-healable structures was characterized using the corresponding FTIR spectrum. In the spectrum of PU-SH, the peaks at 1773 and 1708 cm^{-1} correspond to the C═C stretching of the DA adduct and the C═O stretching vibration of *N*,*N*′-(4,4′-diphenylmethane)bismaleimide (BMI), respectively. Additionally, the peak at 750 cm^{-1} for the furfuryl moiety of furfuryl-functionalized polyurethane (PU-FA) disappeared in the spectrum of PU-SH, which again confirms the successful formation of the DA adduct.

Figure 1f,g shows the scanning electron microscopy (SEM) micrograph and the corresponding energy dispersive spectroscopy (EDAX) mapping of the rGO/Fe_3O_4 nanoparticles. The percentage of Fe_3O_4 nanoparticles reduced onto rGO sheets was found to be 38%. Figure 1h shows the corresponding EDAX mapping of elemental Fe on the rGO sheets. It can be seen that Fe is distributed uniformly onto rGO sheets.

Figure 1i,j shows the atomic force microscopy (AFM) topographic images of neat GO and rGO/Fe_3O_4 nanoparticles, respectively. It can be observed that neat GO sheets are quite large in their lateral dimension. However, rGO/Fe_3O_4 nanoparticles on the other hand are comparatively smaller in their lateral dimension because of the high-temperature solvothermal treatment. The height of the neat GO sheet was measured to be about 10 nm, due to overlapping of GO sheets, whereas the

DOI: 10.1021/acsomega.7b01845
ACS Omega 2018, 3, 1137−1146

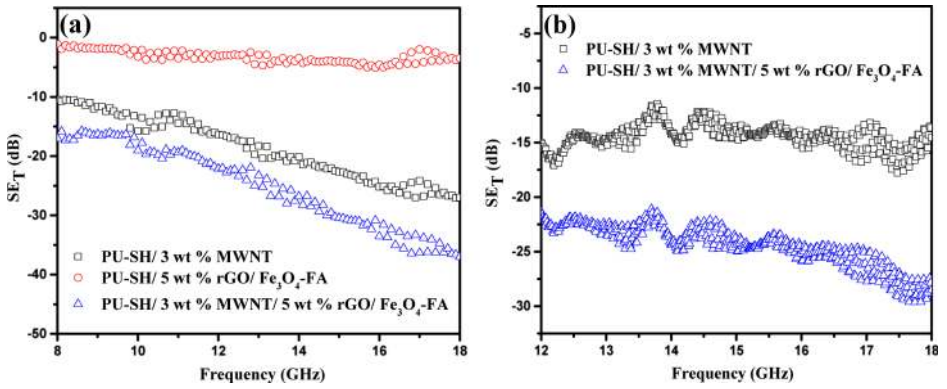

Figure 3. Total SE (SE_T) for (a) 5.8 mm thick toroidal samples and (b) 1 mm thick films.

height of the rGO/Fe_3O_4 sheets was measured to be about 30 nm. The increase in height may be due to grafting of Fe_3O_4 nanoparticles onto GO sheets.

To further confirm the grafting of Fe_3O_4 nanoparticles onto the rGO sheets, XPS spectra were analyzed. From Figure 1i, the XPS survey spectra show the presence of C 1s, O 1s, and Fe 2p peaks at ∼284, 529, and 710 eV, respectively. In the C 1s spectra (shown in the inset), three distinctive peaks at 284.7, 285.5, and 288.6 eV corresponding to C═C, C═O, and O−C═O functional groups, respectively, in GO can be realized. Similarly, in the Fe 2p spectra (shown in the inset), two distinctive peaks at 710.9 and 724.6 eV characteristic of Fe $2p_{3/2}$ and Fe $2p_{1/2}$, respectively, of Fe_3O_4 nanoparticles were realized. The absence of any peak at 719.9 eV confirms the absence of any traces of Fe_2O_3.[42,43]

AC Electrical Conductivity of Nanocomposites. It is envisioned that conductivity is one of the key factors that can enhance the EM wave shielding property of a material. Although conductivity is not the only the criterion for effective EMI shielding, EM wave attenuation can be escalated because of the well-connected MWNT network. MWNTs facilitate charge transport in a well-connected network either by hopping or by tunneling. Intertube distance plays a key role in the conductivity of MWNT-based nanocomposites. Intertube distance can be minimized by increasing the MWNT concentration, which facilitates charge transport through tunneling. In Figure 2a, it can be seen that MWNTs can percolate in the thermoplastic polyurethane matrix at a concentration of as low as 0.5 wt %. At higher loadings of the MWNT, the MWNTs can percolate very well and form effective charge transport networks. In Figure 2b, it can be seen that, when only 5 wt % rGO/Fe_3O_4−FA was added to PU-SH, the conductivity achieved is quite low. This can be attributed to lower conductivity of rGO compared to MWNTs. When both MWNTs and rGO/Fe_3O_4−FA were added together, an improvement in conductivity was again noticed. This can be perceived as an amplification in charge tunneling ability because of the presence of semiconducting MWNTs and partially conducting rGO sheets. The universal power law fitting onto frequency-dependent AC conductivity curves reveals the equivalent number of resistors and capacitive network taking part in the charge transport mechanism of these nanocomposites[44]

$$\sigma'(\omega) = \sigma(0) + \sigma_{AC}(\omega) = \sigma_{DC} + A\omega^s \quad (1)$$

The value of the exponent "*s*" gives an indication of the extent of charge transfer that is taking place through tunneling. In Figure 2, a value of above 0.75 was achieved for the exponent "*s*", which indicates 25 and 75% equivalent network of capacitors and resistances, respectively, for both PU-SH/3 wt % MWNT and PU-SH/3 wt % MWNT/5 wt % rGO/Fe_3O_4−FA. Capacitive networks create virtual connections between MWNTs at high frequencies, due to intertube polarization, thereby leading to amplification of conductivity at high frequencies, where DC conductivity has not yet reached.[45]

Microwave Shielding Ability of Nanocomposites. The EMI shielding efficiency of a material is quantified as the ratio of the intensities of the incident wave to that of the transmitted wave. The attenuation of the incident EM wave is manifested as the total SE (SE_T) and is expressed in decibels (dB). The total SE is a culmination of the contributions from shielding due to three different scattering mechanisms, namely, reflection from the rear surface of the shield, attenuation by absorption as the wave passes through the shield, and multiple reflections, which is neglected because it occurs only in materials with thickness less than its skin depth and whatever wave is reflected from the inner surface of the shield will eventually get absorbed. It is apparent that shielding by absorption is always the most preferred mechanism of shielding. Shielding by absorption is brought about by the magnetic and electric dipoles in the shield that can interact with the magnetic and electric fields, respectively, of the incident EM wave.

In a two-port VNA, SE is measured in terms of various scattering parameters (S_{11}, S_{22}, S_{12}, and S_{21}); therefore[46]

$$SE_T = 10 \log \left| \frac{1}{S_{12}} \right|^2 \quad (2)$$

$$SE_R = 10 \log \left| \frac{1}{(1 - S_{11}{}^2)} \right| \quad (3)$$

$$SE_A = 10 \log \left| \frac{1 - S_{11}{}^2}{S_{12}{}^2} \right| \quad (4)$$

Figure 3a represents the total SE of nanocomposite samples of about 5.8 mm in thickness. Because SE scales with MWNT concentration, with only 3 wt % loading of conducting MWNTs, a SE_T of −27 dB was achieved at 18 GHz. MWNTs help in attenuating EM waves not only because of its conducting nature but also because they promote Ohmic losses through charge transport.[3] EMI shielding is enhanced by a very well-connected MWNT network. With the increase in the MWNT concentration, multiple scattering occurs within

DOI: 10.1021/acsomega.7b01845
ACS Omega 2018, 3, 1137−1146

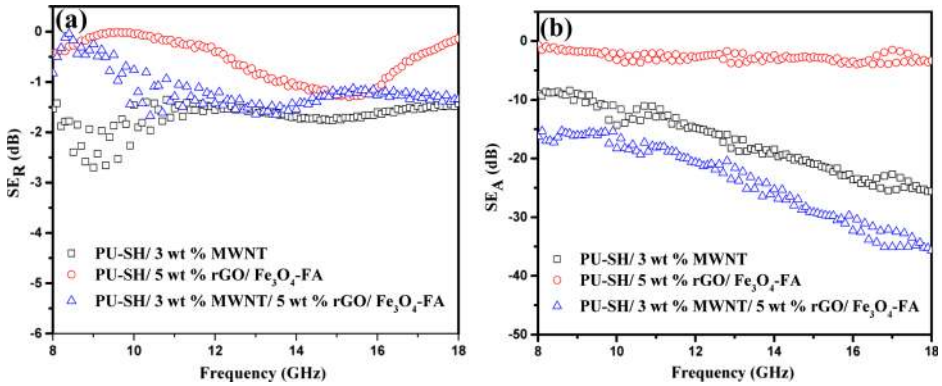

Figure 4. SE due to (a) reflection (SE_R) and (b) absorption (SE_A) for 5.8 mm thick toroidal samples.

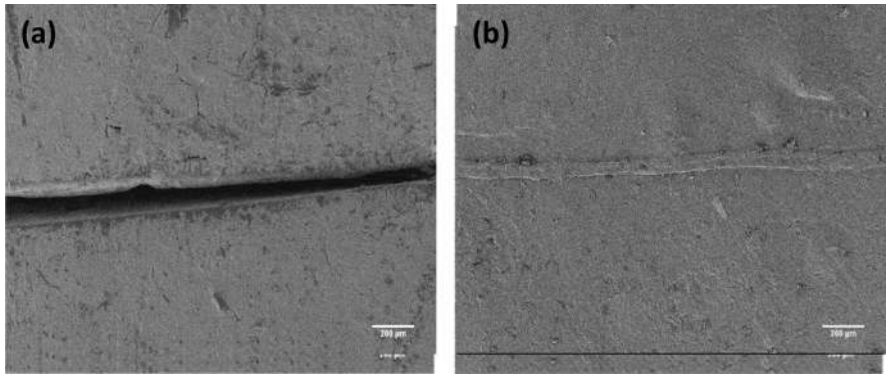

Figure 5. SEM images for self-healing tests on molded samples showing (a) cut sample and (b) healed cut after heating in a microwave oven.

the various overlapping MWNT interfaces and eventually attenuation of the EM waves takes place because of their large specific area. This causes the EM wave shielding by MWNTs to be manifested as absorption. Absorption in the intrinsically conducting and nonmagnetic MWNTs may also be caused because of the presence of defects and intertube polarization (electric dipoles).[47]

When 5 wt % of rGO/Fe_3O_4−FA was introduced, it was realized that the SE_T diminished to a value of −4 dB at 18 GHz. Therefore, it can be said that rGO/Fe_3O_4−FA alone is ineffective in attenuating EM waves because of its poor conductivity and inefficient charge transfer. However, when a 3 wt % MWNT was introduced along with 5 wt % of rGO/Fe_3O_4−FA, a synergistic effect was realized. The SE_T, increased to −36.7 dB at 18 GHz. This observed synergism was due to the nanoscopic nature of MWNTs and rGO/Fe_3O_4, leading to interparticle scattering and absorption. The presence of heterogeneities and macroscopic boundaries in the shield leads to nomadic charge transfer and charge trapping, thereby promoting EM wave absorption.[48]

Figure 3b represents the SE_T of 1 mm thin nanocomposite films. It was realized that even at such small thickness of the shield, the EM wave shielding of above 95% (SE_T of −15 dB) was achieved with only 3 wt % MWNTs. When both MWNTs and rGO/Fe_3O_4−FA were added, attenuation of above 99.7%, that is, SE_T of −28 dB was achieved. Therefore, the proposed shield can be very well used as an effective EM wave absorber and a self-healable coating.

Underlying Mechanism of Microwave Shielding of Nanocomposites. In a two-port VNA, the different *S*-parameters generated help to determine the contribution of absorption and reflection toward the total SE. The SE due to reflection and absorption has been represented in Figure 4a,b, respectively. As mentioned earlier, when it comes to the mechanism of shielding by MWNTs, a small portion of the EM wave gets reflected at the front surface of the shield, but because of enhanced charge transport taking place in the MWNTs, the wave gets attenuated as it passes through the shield by multiple scattering and ohmic losses, which is interpreted by the VNA as absorption. In the case of nanocomposites, 3 wt % MWNTs, SE_R is about −1.5 dB and SE_A is −25.5 dB. This proves that in a well-percolated MWNT network, absorption is the predominant mechanism of shielding. Nanocomposites containing only rGO/Fe_3O_4 show SE_R of only −0.1 dB and the corresponding SE_A show −3.9 dB. This absorption may come from the magnetic Fe_3O_4 nanoparticles which interact with the magnetic component of the EM wave, causing attenuation, from the interconnected rGO network which is slightly conducting causing multiple scattering or due to the charge accumulation at the heterojunctions and interfaces.

As was discussed earlier, a combination of MWNTs and rGO/Fe_3O_4 leads to a synergistic effect which helps in attenuating EM waves by absorption through better impedance matching. From Figure 4, it can be realized that the synergism leads to enhanced EM wave absorption of about −35.4 dB and diminished reflection of only −1.3 dB.

From the above discussion, it can be concluded that the synergism achieved by loading both MWNTs and rGO/Fe_3O_4 is desirable to achieve the maximum possible EM wave absorption.[49,50] The mechanism of shielding can be further analyzed using complex microwave properties such as complex permeability and permittivity. These properties have been discussed in detail in the Supporting Information.

DOI: 10.1021/acsomega.7b01845
ACS Omega 2018, 3, 1137−1146

Scheme 1. Self-Healing Process of Nanocomposites after Heating to 65 °C Using a Microwave Oven (the Inset Illustrates the DA Click Chemistry)

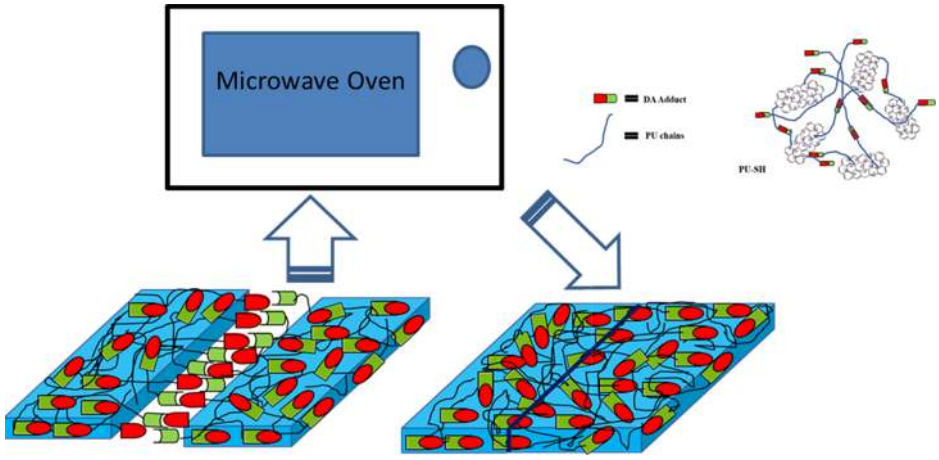

Scheme 2. Synthesis of rGO/Fe_3O_4−FA

Microwave-Healing Ability of Nanocomposites. The microwave shielding nanocomposites developed in the current study were fabricated such that these materials could be used as self-healable coatings for electronic applications. As discussed earlier, furfuryl-linked rGO/Fe_3O_4 (rGO/Fe_3O_4−FA) and PU (PU-FA) were covalently cross-linked using BMI through the DA chemistry. This resulted in nanocomposites with self-healing properties using microwaves. The proposed material apart from being an excellent EMI shielding material also works as a self-healing material because of its microwave absorbing nature. The self-healing ability is triggered by the heat generated in the material as a result of microwave absorption. The absorbed microwave is dissipated across the material in the form of heat.

To demonstrate the self-healing ability of these nanocomposites, samples were made by molding the samples into thin films by compression molding. The film was then cut into two halves and then joined together with slight pressure. As shown in Figure 5a, a cut was made on the film. The joined film was allowed to heal by exposing it to waves from a domestic microwave having a wattage of 900 W for 10 min. After 10 min, the sample was removed from the microwave and observed under a microscope. As shown in Figure 5b, the cut healed completely. As opposed to the conventional hot-air oven, where healing of the cracks may take up to 24 h, healing using a microwave is a much faster and efficient process.[51]

The mechanism of healing has been represented schematically in Scheme 1. The healing of the cut was brought about by the recombination of furan and maleimide groups to form the DA adduct. The DA bond being much weaker compared to other types of covalent bonds can break because of stretching or scratching of these bonds.[41,51] When the cut is heated using microwaves, the heat generated due to the absorption of microwaves by the microwave absorbers in the sample leads to fusing and recombination of these bonds, thereby healing the cut.

CONCLUSIONS

The current study was focused on developing self-healable EMI shielding materials. The nanocomposites developed by cross-linking furfuryl-functionalized rGO/Fe_3O_4 with furfuryl-functionalized PU using BMI and DA chemistry showed self-healing properties when heated using microwave irradiation. The microwave absorbers in the nanocomposite helped in absorbing most of the incoming microwave radiations, and this manifested in exceptional microwave shielding properties. The material when used in the form of 1 mm thin coatings/films provided above 99% microwave screening ability. Substantially, this current work not only verifies the microwave shielding ability of the developed nanocomposites but also verifies that the absorbed microwave when dissipated as heat can be used to heal cuts and scratches in the material.

EXPERIMENTAL SECTION

Materials. Polyethylene glycol (PEG, M_n = 4000 g mol^{-1}) was procured from Merck. 4,4-Diphenylmethane diisocyanate (MDI, 99%), FA, and (BMI) were purchased from Sigma-Aldrich. Pristine MWNTs were purchased from Nanocyl. GO was purchased from BT Corp. Other chemicals and solvents used were obtained from commercial sources.

DOI: 10.1021/acsomega.7b01845
ACS Omega 2018, 3, 1137−1146

Scheme 3. (a) DA Reaction between FA and BMI. (b) Synthesis of PU-FA. (c) Fabrication of PU-SH

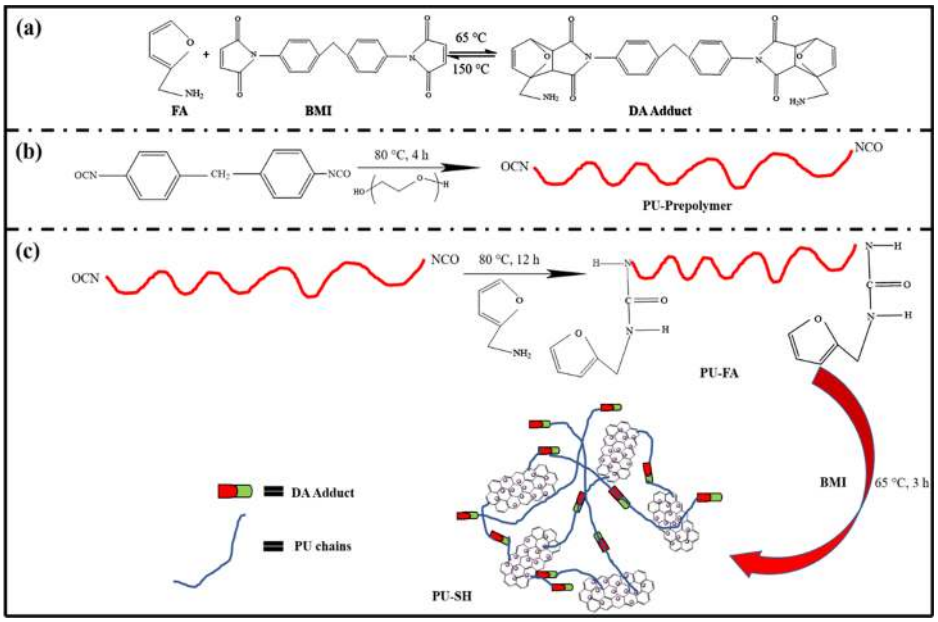

Preparation of rGO/Fe_3O_4 Nanoparticles by the Solvothermal Method. The reduction of magnetic Fe_3O_4 nanoparticles onto rGO sheets was achieved using a one-pot solvothermal method.[52] In a typical procedure, 100 mg of GO was first dispersed in 30 mL ethylene glycol (EG), by probe and bath sonication. 200 mg of $FeCl_3 \cdot 6H_2O$ was dissolved in 10 mL of EG. To this solution, predetermined amount of urea was added and dissolved under magnetic stirring. The as-prepared GO solution was added subsequently to the above solution followed by stirring for 20 min. To this solution, 2 mL of hydrazine hydrate was added and stirred for another 20 min. This solution was transferred to a Teflon-lined autoclave, and solvothermal reduction was carried out at 180 °C for 10 h. After that, the solution was allowed to cool to room temperature, and rGO/Fe_3O_4 was magnetically separated and washed thoroughly with ethanol, followed by drying at 60 °C for 12 h.

Synthesis of FA-Modified rGO/Fe_3O_4 (rGO/Fe_3O_4−FA) Nanoparticles. As shown in Scheme 2, 100 mg of rGO/Fe_3O_4 was dispersed in 100 mL water. pH was adjusted to 1 by adding few drops of HCl. Then, 1 g of FA was added, and the reaction was carried out at 80 °C for 12 h. The obtained product was washed thoroughly with water to remove redundant HCl and unreacted FA and dried under vacuum at 60 °C for 12 h.[41]

Synthesis of PU-FA. PU-FA was synthesized by a two-step process.[51] The first step is the synthesis of PU. In a typical process, 1 mol PEG and 2 mol MDI were dissolved in dimethylformamide (DMF) separately. The two solutions were mixed together and stirred at room temperature for 1 h. The temperature was then increased to 80 °C, and the reaction was carried out for 4 h under nitrogen atmosphere. To this solution, 1 mL of FA was added, and the reaction was carried out for another 4 h. The obtained solution was dried first in air and then under vacuum at 80 °C for 24 h (Scheme 3).

Fabrication of Microwave Shielding Self-Healing PU Nanocomposites. Self-healable PU nanocomposites, capable of microwave shielding, was fabricated by adding 5 wt % of rGO/Fe_3O_4−FA to the PU-FA solution in DMF followed by bath sonication for 30 min. The solution was subjected to mechanical mixing along with sonication for 2 h. To this solution, 1 g of BMI was added, and mechanical stirring was continued at 65 °C for 3 h. To further improve the EMI shielding performance of these nanocomposites, 3 wt % MWNTs was added to these nanocomposites. The solution was then poured into a Teflon-lined Petri plate and dried in air for 24 h followed by vacuum drying for 48 h. Unfilled self-healable PU (PU-SH), PU-SH with 3 wt % MWNT and PU-SH with 5 wt % rGO/Fe_3O_4−FA was prepared as per the above protocol as control samples.

■ ASSOCIATED CONTENT

Supporting Information

The Supporting Information is available free of charge on the ACS Publications website at DOI: 10.1021/acsomega.7b01845.

Mechanism of EMI shielding and various EM parameters such as complex permittivity, complex permeability, and attenuation constant of the composites (PDF)

■ AUTHOR INFORMATION

Corresponding Author

*E-mail: sbose@iisc.ac.in (S.B.).

ORCID

Giridhar Madras: 0000-0003-2211-5055

Suryasarathi Bose: 0000-0001-8043-9192

Notes

The authors declare no competing financial interest.

■ ACKNOWLEDGMENTS

The authors would like to acknowledge the Department of Science and Technology (DST), India, and JATP (IISc) for providing financial aid.

■ REFERENCES

(1) Al-Saleh, M. H.; Sundararaj, U. Electromagnetic interference shielding mechanisms of CNT/polymer composites. *Carbon* **2009**, *47*, 1738−1746.

DOI: 10.1021/acsomega.7b01845
ACS Omega 2018, 3, 1137−1146

(2) Yang, Y.; Gupta, M. C.; Dudley, K. L.; Lawrence, R. W. Novel Carbon Nanotube−Polystyrene Foam Composites for Electromagnetic Interference Shielding. *Nano Lett.* **2005**, *5*, 2131−2134.
(3) Chung, D. D. L. Electromagnetic interference shielding effectiveness of carbon materials. *Carbon* **2001**, *39*, 279−285.
(4) Pawar, S. P.; Biswas, S.; Kar, G. P.; Bose, S. High frequency millimetre wave absorbers derived from polymeric nanocomposites. *Polymer* **2016**, *84*, 398−419.
(5) Kumar, G. S.; Vishnupriya, D.; Joshi, A.; Datar, S.; Patro, T. U. Electromagnetic interference shielding in 1-18 GHz frequency and electrical property correlations in poly(vinylidene fluoride)-multi-walled carbon nanotube composites. *Phys. Chem. Chem. Phys.* **2015**, *17*, 20347−20360.
(6) Geetha, S.; Kumar, K. K. S.; Rao, C. R. K.; Vijayan, M.; Trivedi, D. C. EMI shielding: Methods and materials—A review. *J. Appl. Polym. Sci.* **2009**, *112*, 2073−2086.
(7) Han, J.; Wang, X.; Qiu, Y.; Zhu, J.; Hu, P. Infrared-transparent films based on conductive graphene network fabrics for electromagnetic shielding. *Carbon* **2015**, *87*, 206−214.
(8) Liang, J.; Wang, Y.; Huang, Y.; Ma, Y.; Liu, Z.; Cai, J.; Zhang, C.; Gao, H.; Chen, Y. Electromagnetic interference shielding of graphene/epoxy composites. *Carbon* **2009**, *47*, 922−925.
(9) Cao, M.-S.; Wang, X.-X.; Cao, W.-Q.; Yuan, J. Ultrathin graphene: electrical properties and highly efficient electromagnetic interference shielding. *J. Mater. Chem. C* **2015**, *3*, 6589−6599.
(10) Kar, G. P.; Biswas, S.; Rohini, R.; Bose, S. Tailoring the dispersion of multiwall carbon nanotubes in co-continuous PVDF/ABS blends to design materials with enhanced electromagnetic interference shielding. *J. Mater. Chem. A* **2015**, *3*, 7974−7985.
(11) Srivastava, R. K.; Xavier, P.; Gupta, S. N.; Kar, G. P.; Bose, S.; Sood, A. K. Excellent Electromagnetic Interference Shielding by Graphene- MnFe2O4-Multiwalled Carbon Nanotube Hybrids at Very Low Weight Percentage in Polymer Matrix. *ChemistrySelect* **2016**, *1*, 5995−6003.
(12) Pawar, S. P.; Gandi, M.; Arief, I.; Krause, B.; Pötschke, P.; Bose, S. Graphene Derivatives Doped with Nickel Ferrite Nanoparticles as Excellent Microwave Absorbers in Soft Nanocomposites. *ChemistrySelect* **2017**, *2*, 5984−5999.
(13) Gupta, T. K.; Singh, B. P.; Dhakate, S. R.; Singh, V. N.; Mathur, R. B. Improved nanoindentation and microwave shielding properties of modified MWCNT reinforced polyurethane composites. *J. Mater. Chem. A* **2013**, *1*, 9138−9149.
(14) Gupta, T. K.; Singh, B. P.; Teotia, S.; Katyal, V.; Dhakate, S. R.; Mathur, R. B. Designing of multiwalled carbon nanotubes reinforced polyurethane composites as electromagnetic interference shielding materials. *J. Polym. Res.* **2013**, *20*, 169.
(15) Zhu, J.; Wei, S.; Haldolaarachchige, N.; Young, D. P.; Guo, Z. Electromagnetic Field Shielding Polyurethane Nanocomposites Reinforced with Core−Shell Fe−Silica Nanoparticles. *J. Phys. Chem. C* **2011**, *115*, 15304−15310.
(16) Liu, Z.; Bai, G.; Huang, Y.; Ma, Y.; Du, F.; Li, F.; Guo, T.; Chen, Y. Reflection and absorption contributions to the electromagnetic interference shielding of single-walled carbon nanotube/polyurethane composites. *Carbon* **2007**, *45*, 821−827.
(17) Durmus, Z.; Durmus, A.; Bektay, M. Y.; Kavas, H.; Unver, I. S.; Aktas, B. Quantifying structural and electromagnetic interference (EMI) shielding properties of thermoplastic polyurethane−carbon nanofiber/magnetite nanocomposites. *J. Mater. Sci.* **2016**, *51*, 8005−8017.
(18) Ramôa, S. D. A. S.; Barra, G. M. O.; Oliveira, R. V. B.; de Oliveira, M. G.; Cossa, M.; Soares, B. G. Electrical, rheological and electromagnetic interference shielding properties of thermoplastic polyurethane/carbon nanotube composites. *Polym. Int.* **2013**, *62*, 1477−1484.
(19) Cao, M.-S.; Yang, J.; Song, W.-L.; Zhang, D.-Q.; Wen, B.; Jin, H.-B.; Hou, Z.-L.; Yuan, J. Ferroferric Oxide/Multiwalled Carbon Nanotube vs Polyaniline/Ferroferric Oxide/Multiwalled Carbon Nanotube Multiheterostructures for Highly Effective Microwave Absorption. *ACS Appl. Mater. Interfaces* **2012**, *4*, 6949−6956.
(20) Ganzhorn, M.; Klyatskaya, S.; Ruben, M.; Wernsdorfer, W. Carbon Nanotube Nanoelectromechanical Systems as Magnetometers for Single-Molecule Magnets. *ACS Nano* **2013**, *7*, 6225−6236.
(21) Izu, Y.; Shiomi, J.; Takagi, Y.; Okada, S.; Maruyama, S. Growth Mechanism of Single-Walled Carbon Nanotube from Catalytic Reaction Inside Carbon Nanotube Template. *ACS Nano* **2010**, *4*, 4769−4775.
(22) Subianto, S.; Dutta, N. K.; Choudhury, N. R. Water-Reprocessable, Reformable, and Ecofriendly Sustainable Material Based on Disulfide-Cross-Linked Polyethyleneimine. *ACS Omega* **2017**, *2*, 3036−3042.
(23) Rathi, P.; Jha, M. K.; Hata, K.; Subramaniam, C. Real-Time, Wearable, Biomechanical Movement Capture of Both Humans and Robots with Metal-Free Electrodes. *ACS Omega* **2017**, *2*, 4132−4142.
(24) Song, E.-H.; Cho, K.-I.; Kim, H.-E.; Jeong, S.-H. Biomimetic Coating of Hydroxyapatite on Glycerol Phosphate-Conjugated Polyurethane via Mineralization. *ACS Omega* **2017**, *2*, 981−987.
(25) Fu, X.; Wang, Y.; Zhong, W.-H.; Cao, G. A Multifunctional Protein Coating for Self-Assembled Porous Nanostructured Electrodes. *ACS Omega* **2017**, *2*, 1679−1686.
(26) Pramanik, A.; Jones, S.; Pedraza, F.; Vangara, A.; Sweet, C.; Williams, M. S.; Ruppa-Kasani, V.; Risher, S. E.; Sardar, D.; Ray, P. C. Fluorescent, Magnetic Multifunctional Carbon Dots for Selective Separation, Identification, and Eradication of Drug-Resistant Superbugs. *ACS Omega* **2017**, *2*, 554−562.
(27) Qi, W.; Yan, J.; Sun, H.; Wang, H. Multifunctional Nanocomposite Films for Synergistic Delivery of bFGF and BMP-2. *ACS Omega* **2017**, *2*, 899−909.
(28) Yang, P.; Yang, W. Hydroxylation of Organic Polymer Surface: Method and Application. *ACS Appl. Mater. Interfaces* **2014**, *6*, 3759−3770.
(29) Gao, A.; Wu, Q.; Wang, D.; Ha, Y.; Chen, Z.; Yang, P. A Superhydrophobic Surface Templated by Protein Self-Assembly and Emerging Application toward Protein Crystallization. *Adv. Mater.* **2016**, *28*, 579−587.
(30) Wang, D.; Ha, Y.; Gu, J.; Li, Q.; Zhang, L.; Yang, P. 2D Protein Supramolecular Nanofilm with Exceptionally Large Area and Emergent Functions. *Adv. Mater.* **2016**, *28*, 7414−7423.
(31) Tao, F.; Han, Q.; Liu, K.; Yang, P. Tuning Crystallization Pathways through the Mesoscale Assembly of Biomacromolecular Nanocrystals. *Angew. Chem., Int. Ed.* **2017**, *56*, 13440−13444.
(32) Yue, C.; Sun, H.; Liu, W.-J.; Guan, B.; Deng, X.; Zhang, X.; Yang, P. Environmentally Benign, Rapid, and Selective Extraction of Gold from Ores and Waste Electronic Materials. *Angew. Chem., Int. Ed.* **2017**, *56*, 9331−9335.
(33) Kavitha, A. A.; Singha, N. K. "Click Chemistry" in Tailor-Made Polymethacrylates Bearing Reactive Furfuryl Functionality: A New Class of Self-Healing Polymeric Material. *ACS Appl. Mater. Interfaces* **2009**, *1*, 1427−1436.
(34) Willocq, B.; Bose, R. K.; Khelifa, F.; Garcia, S. J.; Dubois, P.; Raquez, J.-M. Healing by the Joule effect of electrically conductive poly(ester-urethane)/carbon nanotube nanocomposites. *J. Mater. Chem. A* **2016**, *4*, 4089−4097.
(35) Chen, X.; Dam, M. A.; Ono, K.; Mal, A.; Shen, H.; Nutt, S. R.; Sheran, K.; Wudl, F. A Thermally Re-mendable Cross-Linked Polymeric Material. *Science* **2002**, *295*, 1698−1702.
(36) Pramanik, N. B.; Singha, N. K. Direct functionalization of multi-walled carbon nanotubes (MWCNTs) via grafting of poly(furfuryl methacrylate) using Diels-Alder "click chemistry" and its thermoreversibility. *RSC Adv.* **2015**, *5*, 94321−94327.
(37) Liu, Y.-L.; Chuo, T.-W. Self-healing polymers based on thermally reversible Diels-Alder chemistry. *Polym. Chem.* **2013**, *4*, 2194−2205.
(38) Nasrollahzadeh, M.; Maham, M.; Rostami-Vartooni, A.; Bagherzadeh, M.; Sajadi, S. M. Barberry fruit extract assisted in situ green synthesis of Cu nanoparticles supported on a reduced graphene oxide-Fe3O4 nanocomposite as a magnetically separable and reusable catalyst for the O-arylation of phenols with aryl halides under ligand-free conditions. *RSC Adv.* **2015**, *5*, 64769−64780.

DOI: 10.1021/acsomega.7b01845
ACS Omega 2018, 3, 1137−1146

(39) Chen, T.; Qiu, J.; Zhu, K.; Che, Y.; Zhang, Y.; Zhang, J.; Li, H.; Wang, F.; Wang, Z. Enhanced electromagnetic wave absorption properties of polyaniline-coated Fe3O4/reduced graphene oxide nanocomposites. *J. Mater. Sci.: Mater. Electron.* **2014**, *25*, 3664−3673.
(40) Pawar, S. P.; Gandi, M.; Bose, S. High performance electromagnetic wave absorbers derived from PC/SAN blends containing multiwall carbon nanotubes and Fe3O4 decorated onto graphene oxide sheets. *RSC Adv.* **2016**, *6*, 37633−37645.
(41) Li, J.; Zhang, G.; Sun, R.; Wong, C.-P. A covalently cross-linked reduced functionalized graphene oxide/polyurethane composite based on Diels-Alder chemistry and its potential application in healable flexible electronics. *J. Mater. Chem. C* **2017**, *5*, 220−228.
(42) Mondal, S.; Rana, U.; Malik, S. Reduced Graphene Oxide/Fe3O4/Polyaniline Nanostructures as Electrode Materials for an All-Solid-State Hybrid Supercapacitor. *J. Phys. Chem. C* **2017**, *121*, 7573−7583.
(43) Saha, S.; Jana, M.; Samanta, P.; Murmu, N. C.; Kim, N. H.; Kuila, T.; Lee, J. H. Hydrothermal synthesis of Fe3O4/RGO composites and investigation of electrochemical performances for energy storage applications. *RSC Adv.* **2014**, *4*, 44777−44785.
(44) Ngai, K. L.; Jonscher, A. K.; White, C. T. On the origin of the universal dielectric response in condensed matter. *Nature* **1979**, *277*, 185−189.
(45) Thomassin, J.-M.; Jérôme, C.; Pardoen, T.; Bailly, C.; Huynen, I.; Detrembleur, C. Polymer/carbon based composites as electromagnetic interference (EMI) shielding materials. *Mater. Sci. Eng., R* **2013**, *74*, 211−232.
(46) Pawar, S. P.; Bhingardive, V.; Jadhav, A.; Bose, S. An efficient strategy to develop microwave shielding materials with enhanced attenuation constant. *RSC Adv.* **2015**, *5*, 89461−89471.
(47) Pawar, S. P.; Gandi, M.; Saraf, C.; Bose, S. Exceptional microwave absorption in soft polymeric nanocomposites facilitated by engineered nanostructures. *J. Mater. Chem. C* **2016**, *4*, 4954−4966.
(48) Mural, P. K. S.; Pawar, S. P.; Jayanthi, S.; Madras, G.; Sood, A. K.; Bose, S. Engineering Nanostructures by Decorating Magnetic Nanoparticles onto Graphene Oxide Sheets to Shield Electromagnetic Radiations. *ACS Appl. Mater. Interfaces* **2015**, *7*, 16266−16278.
(49) Pawar, S. P.; Stephen, S.; Bose, S.; Mittal, V. Tailored electrical conductivity, electromagnetic shielding and thermal transport in polymeric blends with graphene sheets decorated with nickel nanoparticles. *Phys. Chem. Chem. Phys.* **2015**, *17*, 14922−14930.
(50) Chaudhary, A.; Kumar, R.; Teotia, S.; Dhawan, S. K.; Dhakate, S. R.; Kumari, S. Integration of MCMBs/MWCNTs with Fe3O4 in a flexible and light weight composite paper for promising EMI shielding applications. *J. Mater. Chem. C* **2017**, *5*, 322−332.
(51) Li, J.; Zhang, G.; Deng, L.; Zhao, S.; Gao, Y.; Jiang, K.; Sun, R.; Wong, C. In situ polymerization of mechanically reinforced, thermally healable graphene oxide/polyurethane composites based on Diels-Alder chemistry. *J. Mater. Chem. A* **2014**, *2*, 20642−20649.
(52) Cao, W.; Ma, Y.; Zhou, W.; Guo, L. One-pot hydrothermal synthesis of rGO-Fe3O4 hybrid nanocomposite for removal of Pb(II) via magnetic separation. *Chem. Res. Chin. Univ.* **2015**, *31*, 508−513.

DOI: 10.1021/acsomega.7b01845
ACS Omega 2018, 3, 1137−1146